# Finite Elements Analysis and Optimisation of Robotic Arm Under Dynamic Loads

**Sandeep Chowdhry[1]**

[1]Engineering Consultant & Trainer, Chandigarh, India

---

**Abstract –** *To design a high-performance Robotic Arm, it is essential to analyse it under dynamic loads. This study aims to explore the structural strength of the Robotic Arm under dynamic load, optimise the weight and evaluate the optimised design. Dynamic simulation of Robotic Arm is performed using Auto Desk Professional (AIP). In addition, Finite Element Analysis (FEA) is performed on the Robotic Arm under dynamic loads. Response Surface Method (RSM) is used for optimisation. The data is analysed using graphs, descriptive statistics and inferential statistics. The results show that the maximum resultant moment on revolute joint 1 is more than five times that on revolute joint 2. The optimisation led to 50.17% and 32.93% reduction in the safety of factor link 1 and link 2, respectively. The thickness of link 1 has a more considerable effect on the safety factor and mass than its cross-section area The overall mass of the Robotic Arm is reduced by 36.69%. The optimised Robotic Arm's first natural frequency is more than three times the maximum design frequency. The maximum stress produced in the Robotic Arm is well below the yield strength of the Aluminium-6061. It is concluded that the high structural stability of the base and link 1 are essential to improve the performance of the Robotic Arm. Boundary conditions may be selected according to the actual working environment to get more accurate FEA results. There is a possibility of using materials with yield strength lower than Aluminium-6061.*

***Key Words*****:** Dynamic Simulation, FEA, RSM, Modal Analysis

## 1. INTRODUCTION

This study continues the research to design a Robotic Arm for tracking and force control for education [1]. It is essential to perform the structural design analysis under the dynamic loads as it considers the effect of joint positions, velocities, accelerations and reaction forces. These reaction forces help test the components similar to the actual working environment. The weight is a prime optimisation parameter, and structural optimisation can be categorised as sizing, shape, and topology optimisation [2]. The finite Element Method (FEM) in modal analysis results show that an increase in preload force leads to a decrease in natural frequencies at a low level [3]. These findings are in agreement with the experimental results [4]. Therefore, the main aim of this study is 1) To analyse the structural strength of the Robotic Arm under dynamic loading; 2) To perform structural optimisation to reduce weight; 3) To evaluate the optimised design for high structural vibration frequencies. This study intends to contribute to the literature on structural design optimisation under dynamic loading.

## 2. DYNAMIC SIMULATION

Autodesk Inventor Professional (AIP) 2016 is used to create the Robotic Arm assembly, as shown in Fig. 1. The detailed mechanism of connection of motors to link 1 and link 2 is not shown. Aluminium-6061 is assigned to the Robotic Arm. The base is fixed. In a dynamic simulation environment, revolute joint 1 is created between the base and link 1. A revolute joint is created between link 1 and link 2. Revolute joint 3 is created between link 2 and gripper. Gravity load is apllied in the vertically downward direction. Electric motors are suppresed in the dynamic analysis as they are mounted on the base.

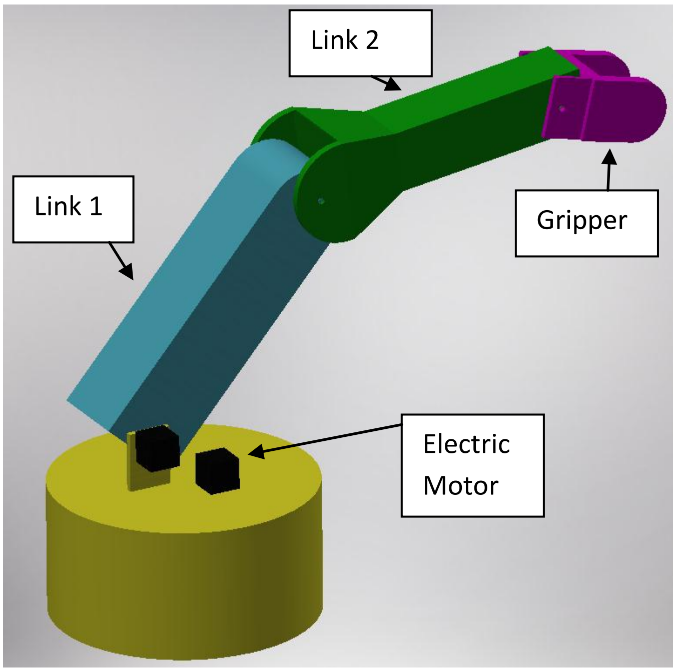


**Fig - 1**: Robotic Arm

### 2.1. Dynamic analysis of link 1

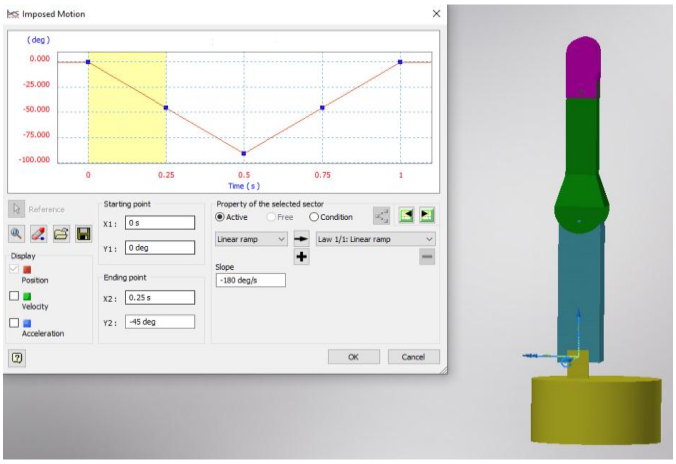

**Fig - 2**: Position graph of revolute joint 1

Fig. 2 show that revolute joint 1 between the base and link 1 is assigned positions of 0°,-45°,-90°,-45°,0° (clockwise rotation) at time of 0 sec, 0.25 sec, 0.5 sec, 0.75 sec and at 1 sec, respectively.

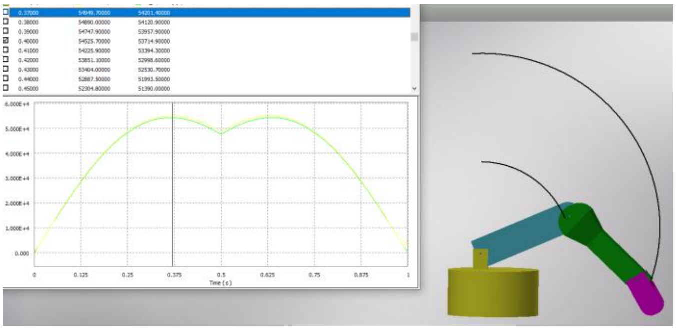

**Fig - 3**: Resultant moment graph of revolute joint 1

The graph in Fig. 3 shows the maximum resultant moment of 54949.76 N.mm on revolute joint 1 at the position of 23.4° with the horizontal plane at time = 0.37 sec. The black lines show the path of travel of revolute joint 2 and revolute joint 3.

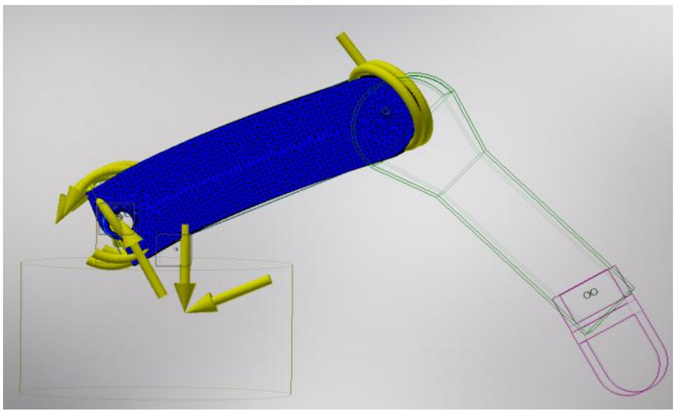

**Fig - 4**: Dynamic loads on link 1 due to revolute joint 1

The applied dynamic loads on link 1 are shown in Fig. 4, such as gravity, body loads, remote force load, moment, remote force, moment 2 calculated by AIP. Maximum stress (34.12 Mpa) concentration is around the hole. The safety factor of the Link1 is 8.08. It indicates that link 1 can operate safely in the work environment.

### 2.2. Dynamic analysis of link 2

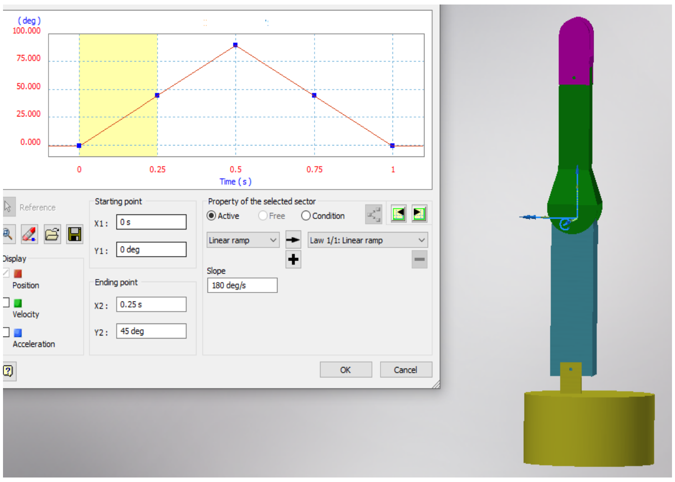

**Fig - 5**: Position graph of revolute joint 2

The revolute joint 2 between link 1 and link 2 is assigned positions of 0°,45°,90°,45°,0° (clockwise rotation) at time of 0 sec, 0.25 sec, 0.5 sec, 0.75 sec and at 1 sec, respectively.

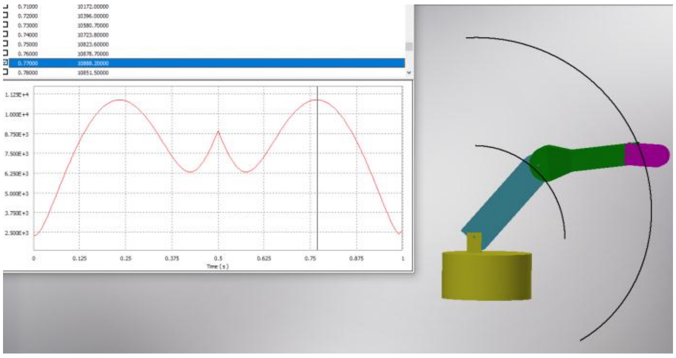

**Fig - 6**: Resultant moment graph of revolute joint 2

The graph in Fig. 6 shows the maximum resultant moment of 10888.2 N.mm on revolute joint 2 at 41.4° with the horizontal plane at time = 0.77 sec.

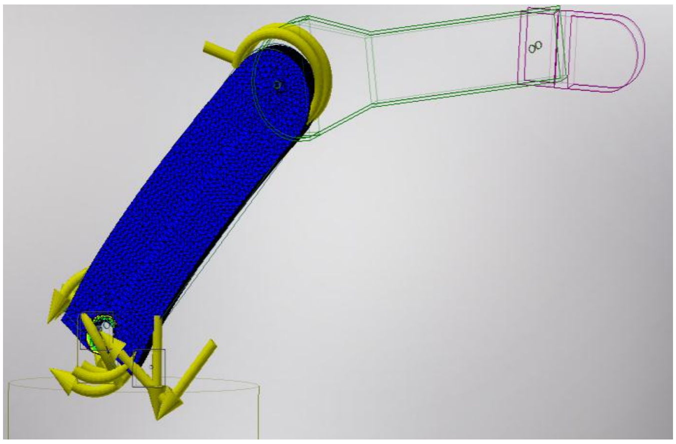

**Fig - 7**: Dynamic loads on link 1 due to revolute joint 2

Link 1 is analysed for the maximum resultant moment at revolute joint 2. The applied dynamic loads shown in Fig. 7 are gravity, body loads, remote force load, moment, and moment 2 calculated by AIP. Maximum Von Mises stress (28.67 Mpa) is concentrated around the hole. The safety factor of the Link1 is 9.59. It indicates that link 1 can operate safely in the work environment.

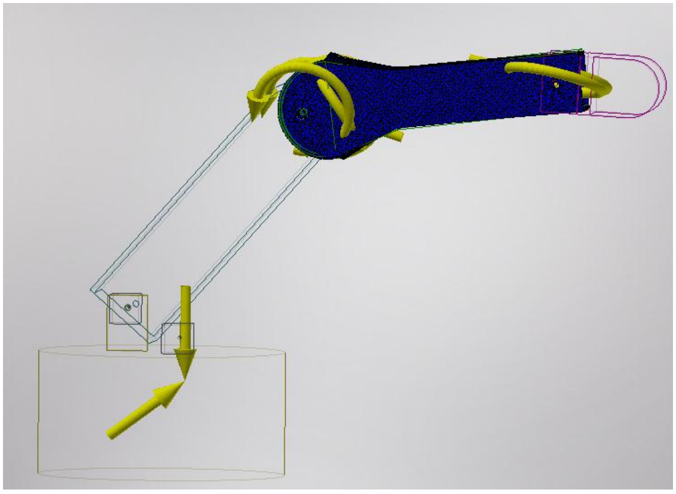

**Fig - 8**: Dynamic loads on link 2 due to revolute joint 2

Link 2 is analysed for the maximum resultant moment at revolute joint 2. The applied dynamic loads shown in Fig. 8 are gravity, body loads, remote force load, moment, and moment 2 calculated by AIP. Maximum Von Mises stress (12.69 Mpa) is concentrated around the hole. The safety factor of Link 2 is 15. It indicates that link 2 can operate safely in the work environment.

### 2.3. Dynamic analysis of gripper

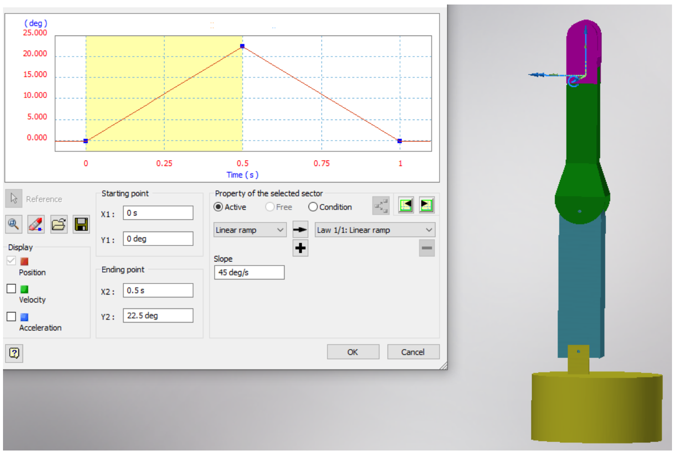

**Fig - 9**: Position graph of revolute joint 3

The Fig. 9 show revolute joint 3 between link 2 and gripper is assigned positions of 0°,90°,0° (clockwise rotation) at time of 0 sec, 0.5 sec and at 1 sec, respectively.

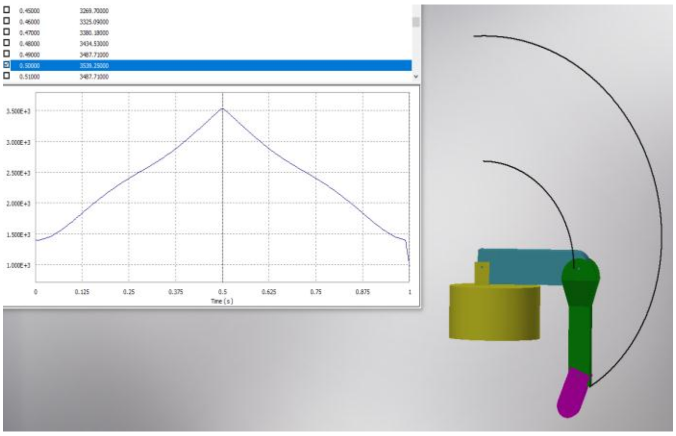

**Fig - 10**: Resultant moment graph of revolute joint 3

The graph in Fig. 10 show the maximum resultant moment of 3539.25 N.mm on revolute joint 3 at the position of 22.5° with the horizontal plane at time = 0.5 sec.

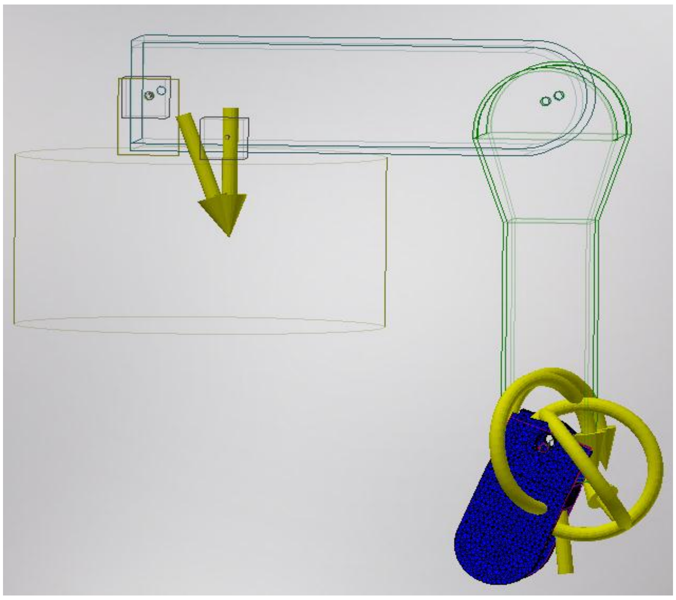

**Fig - 11**: Dynamic loads on gripper due to revolute joint 3

Gripper with no payload is analysed for the maximum resultant moment at revolute joint 3. The applied dynamic loads shown in Fig. 11 are gravity, body loads, remote force load, moment, and moment 2 calculated by AIP. Maximum Von Mises stress (1.17277 Mpa) is concentrated around the hole. The safety factor of the gripper is 15. It indicates that the gripper can operate safely in the work environment.

The safety factor of link 1 at revolute joint 1 and revolute joint 2 is 8.08 and 9.59, respectively. Second, link 2 and the gripper has a safety factor of 15. The variation in the safety factors of the links of the Robotic Arm presents an opportunity for further individual link optimisation agrees with [5]. The Response Surface Method (RSM) is more effective than conventional optimisation algorithms [6][7]. Therefore, RSM is used to optimise link 1. Parametric relations are applied between link 1, link 2 and between link 1 and link 2 ( Link2-Length = Link 1-Length +25mm) to maintain the uniform modification in the link 2 geometry with respect to the link 1 design,. As a result, by changing one dimension of link 1, a new assembly is created with optimised dimensions of link 1 and link 2. The link 2 thickness is independent of the parametric relations. So, link 2 is optimised by varying the thickness and comparing the maximum von mises stress produced with the yield strength (275 Mpa) of Aluminium-6061 to evaluate its structural strength..

## 3. OPTIMISATION

### 3.1 Optimisation invariants

The following parameters are invariant,1) link 1 and link 2 each of length 0.49m; 2) link 1 and link 2 material is aluminium-6061; 3) link 1 and link 2 have square tubular cross-section.

### 3.2 Optimisation variable

The variable parameters are 1) Link 1 cross-section size; 2) The thickness of link 1 and link 2. These variables are optimised to maximise the first natural frequency and minimise the safety factor and mass of the Robotic arm.

### 3.3 Parameters, Levels and Responses

Table 1 shows the level settings of the cross-section of link 1 and thicknesses of link 1 of the robotic arm. The first natural frequency (Hz) and the mass (kg) of the robotic arm is selected as the response.

**Table -1:** Process parameter levels

| Process Parameter | Low Level | High Level |
|---|---|---|
| Link 1 cross-section ($mm^2$) | 110x110 | 130x130 |
| Link 1 (mm) | 4 | 8 |

### 3.4 Optimisation of link 1

Minitab 2019 software is used to design the run order for the Response Surface Method (RSM) . The Central Composite Design (CCD) consists of 8 factorial points and six centre points or 14 points (Run 1-14) with one replicate and two blocks. The CCD is shown in Table 2.

**Table -2:** Central composite design of RSM

| Run Order | Link 1 area ($mm^2$) | Link 1 thickness (mm) |
|---|---|---|
| 1 | 120x120 | 6.0 |
| 2 | 120x120 | 6.0 |
| 3 | 120x120 | 8.83 |
| 4 | 134.14x134.14 | 6.0 |
| 5 | 120x120 | 3.17 |
| 6 | 120x120 | 6.0 |
| 7 | 110x110 | 6.0 |
| 8 | 110x110 | 8.0 |
| 9 | 130x130 | 8.0 |
| 10 | 110x110 | 4.0 |
| 11 | 130x130 | 4.0 |
| 12 | 120x120 | 6.0 |
| 13 | 120x120 | 6.0 |
| 14 | 120x120 | 6.0 |

### 3.5 Procedure

#### 3.5.1 Procedure for link 1

Link 1 is exported from the dynamic simulation environment to the Finite Element Analysis (FEA) environment in AIP to perform stress analysis. The Robotic Arm assembly is assigned Aluminium-6061. A fixed constraint is applied at the end of link 1. Gravity load is applied to the Robotic arm. Mesh element size is 0.025 to get accurate results. In the first run, the cross-section area and thicknesses of link1 are selected as per Table 2. The simulation result of the safety factor and mass of link 1 is recorded. Similarly, the response values are recorded for all the run orders. Afterwards, Minitab software is used to analyse the response surface design with a confidence level of 95% (α=0.05). The residual plots showed that the errors are random, independent, normally distributed and have constant variance across all factor levels.

The analysis of the RSM shows that for safety factor and mass, cross-section of link 1, thickness of link 1, square of link 1 cross-section, sqaure of thickness of link 1 and interaction between cross-section of link 1 and thickness of link 1 are statistically significant at α =0.05.

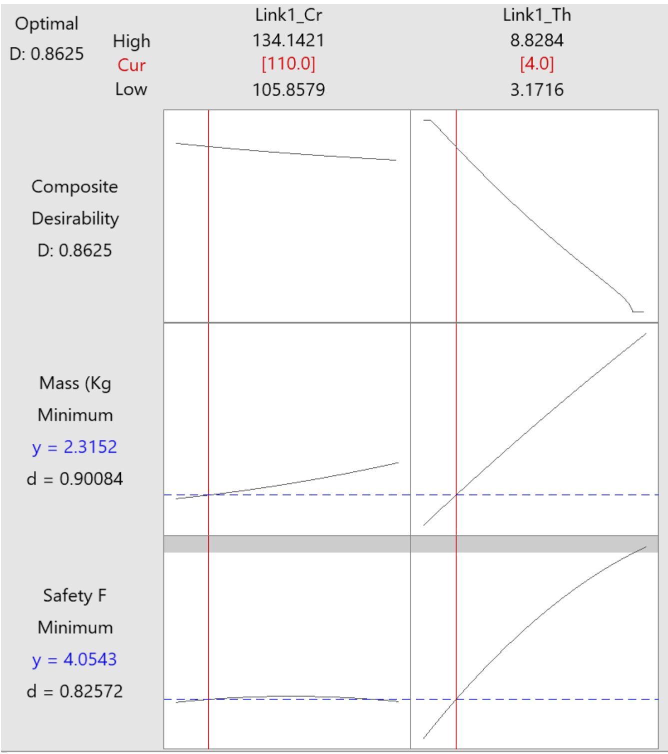


**Fig - 12**: Optimised cross-section area and thicknesses of link 1

Fig.12 show that link 1 square cross-section of 0.11m and link 1 thickness of 4 mm resulted in the safety factor of 4.0543 and mass of 2.3152 Kg for link 1.

#### 3.5.2 Procedure for link 2

Link 2 thickness is independent of the parametric relations. By varying the thickness, the obtained safety factor, mass and maximum Von Mises stress values are recorded as shown in Table 3.

**Table -3:** Process parameter levels

| Thickness of Link 2 (mm) | Min. Safety Factor | Max Von Mises Stress (Mpa) | Mass (Kg) |
|---|---|---|---|
| 1 | 4.94 | 55.69 | 0.52 |
| 2 | 11.02 | 24.96 | 1.02 |
| 3 | 15 | 16.85 | 1.52 |
| 4 | 15 | 12.70 | 2.00 |

Link 2 thickness of 1 mm gave the minimum safety factor of 4.94 and mass of 0.52 Kg. The Maximum von mises stress is 55.69 Mpa and is below the yield stress of Aluminium-6061 of 275 Mpa. It indicates that reducing the link 2 thickness to 1 mm is safe.

## 4. MODAL ANALYSIS OF OPTIMISED ROBOTIC ARM

The optimised design of link 1 has a square cross-section of 0.11m. The square cross-section 0.074m of link 2 is calculated through parametric relations. The same boundary conditions as in [1] are applied. Both the motors are modelled as rigidly connected (cantilever) to the base. The base is modelled as cantilevered to the ground. The fixed base of the Robotic Arm is not used in the FEA for simplification. A fixed constraint is applied at the end of link1. The spring elements representing the pre-tensioned steel band are also cantilevered. The validity and appropriateness of these boundary conditions of this model are addressed in [8][9]. Fig. 13 shows the modal analysis model of the Robotic Arm model with link 1 and link 2 joint angles at 0°,

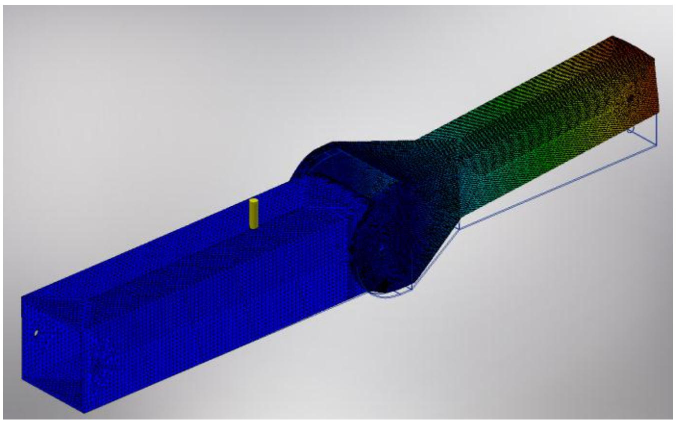

**Fig – 13**: Modal analysis of link 1 and link 2 at 0° joint angle

The optimised design has a first natural frequency is 137.39 Hz. The NEMA 23S stepper motors selected has a maximum speed of 2500 rpm. So, the optimised first natural frequency is more than three times the maximum design vibration frequency (41.67 Hz). The mass of the Robotic Arm is 2.698 Kg.

## 5. DISCUSSION

The dynamic analysis shows that the maximum resultant moment (54949.76 N.mm) acting on revolute joint 1 is five times that acting on revolute joint 2 (10888.2 N.mm). Therefore, care may be taken in designing the base and link 1 to provide optimum structural strength to the Robotic Arm. Second, the optimised cross-section area of link 1 (0.11m) and thickness (0.004 m) reduced the safety factor to 4.0543. It is a 50.17% reduction in the safety factor compared to the minimum safety factor of 8.08 (Fig. 4) obtained by the dynamic analysis. Similarly, reducing the thickness of link 2 from 4 mm to 1 mm reduced the safety factor from 15 to 4.94. It is 32.93% reduction in the safety factor. In addition,the modal analysis result (Fig. 13) show that the overall mass of the Robotic Arm is reduced to 2.698 Kg from 7.3539 Kg [1]. It is 36.69% reduction in the mass of the Robotic Arm. Therefore, it is important to choose the boundary conditions according to the actual working environment to get more accurate FEA results. Third, the first natural frequency (137.39 Hz) of the optimised design of the Robotic Arm is more than three times the maximum design frequency (41.67 Hz). It shows that the Robotic Arm is capable of high performance. In addition, the high slope of the thickness curve in the optimisation graph (Fig. 12) shows that the thickness of link 1 has a more considerable effect on the mass and safety factor than the cross-section area of link 1. As a result, it is possible to further optimise the cross-section area and thickness if the optimum value of the first natural frequency of the Robotic Arm is selected as two times the maximum design vibration frequency of 41.67 Hz. Fourth, the low value of the maximum Von Mises stress in link 1 and link 2 than the yield strength of the Aluminium-6061 (275 Mpa) suggest possibility of using materials that have yield strength less than Aluminium-6061.

## 6. CONCLUSIONS

This research reported the dynamic analysis and optimisation of the Robotic Arm. The study also provided supporting modal analysis data for the Robotic Arm. Detailed findings are summarised here. 1) The maximum resultant moment at revolute joint 1 is five times that at revolute joint 2. Therefore, the high structural strength of the base and link 1 are essential to provide stability and increase the Robotic Arm's performance. 2) Optimisation led to reduction in the safety factor by 50.17% and 32.93% for link 1 and link 2, respectively. In addition, overall mass of the Robotic Arm is reduced by 36.69%. 3) The first natural frequency of the optimised design of the Robotic Arm is more than three times the maximum design frequency. The thickness of link 1 has a more considerable effect on the safety factor and mass link 1 cross-section area. 4) The low value of the maximum von mises stress in link 1 and link 2 than the yield strength of the Aluminium-6061 (275 Mpa) suggests the possibility of using materials that have yield strength less than Aluminium-6061. The limitation of this study is that gripper design has not been optimised with and without payload. A suggested direction for future research is to optimise the gripper's size, shape, material, and mechanism.

## REFERENCES

[1] S. Chowdhry, "Structural Design, Analysis and Optimisation of Robotic Arm," International Research Journal of Engineering and Technology , vol. 9, no. 5, 2022.

[2] Femto Engineering. Structural Design Optimization Techniques & Tools - Femto Engineering. FemtoEngineering, 2017. [Online]. Available: https://www.femto.eu/stories/design-optimization/.

[3] A. Lu, J. Xu, and H. Liu. Effect of a preload force on anchor system frequency. Int. J. Min. Sci. Technol., 2013; 23(1): 135–138.

[4] W. Xu and D. P. Hess. Effect of Fastener Preload on Structural Damping. J. Fail. Anal. Prev., 2013; 13(6): 744–747

[5] G. Kurebwa1, T. Mushiri, Structural Design, Optimisation and Analysis of Robotic Arm Via Finite Elements, Progress in Human Computer Interaction, Volume 1 Issue 2 | 2018, pp 1-9

[6] W. K. Rule. A Response Surface for Structural Optimization. J. Offshore Mech. Arct. Eng., 1997; 119(3): 196

[7] Y. Yanhui, L. Dong, H. Ziyan, and L. Zijian. Optimisation of Preform Shapes by RSM and FEM to Improve Deformation Homogeneity in Aerospace Forgings. Chinese J. Aeronaut., 2010; 23(2): 260–267

[8] J. Roy and L. L. Whitcomb, "Comparative structural analysis of 2-DOF semi-direct-drive linkages for robot arms," IEEE/ASME Trans. Mechatron., vol. 4, pp. 82–86, Mar. 1999.

[9] J. Roy and L. L. Whitcomb, "Structural design optimisation and comparative analysis of a new high-performance robot arm via finite element analysis," Johns Hopkins University, Department of Mechanical Engineering, Dynamics and Control Laboratory, Baltimore, MD, Tech. Rep. 9801, 1998.

**BIOGRAPHIES**

Er. Sandeep Chowdhry has done Bachelor of Engineering in Mechanical Engineering with a Specialisation in Manufacturing Engineering from S.L.I.E.T. Punjab, India and is interested in solving industrial problems and imparting training to the professionals in the industry. Email: studentsuniversityonline@gmail.com